Distribution Agreement

In presenting this thesis as a partial fulfillment of the requirements for a degree from Emory University, I hereby grant to Emory University and its agents the non-exclusive license to archive, make accessible, and display my thesis in whole or in part in all forms of media, now or hereafter now, including display on the World Wide Web. I understand that I may select some access restrictions as part of the online submission of this thesis. I retain all ownership rights to the copyright of the thesis. I also retain the right to use in future works (such as articles or books) all or part of this thesis.

Nikita Patel March 30, 2023

Distribution & Density of 5-HT Fibers in the Lumbar Spinal Cord of the Mouse

by

Nikita Patel

Marie-Claude Perreault
Adviser

Neuroscience & Behavioral Biology

Marie-Claude Perreault

Adviser

Francisco Alvarez

Committee Member

Astrid Prinz

Committee Member

2023

Distribution & Density of 5-HT Fibers in the Lumbar Spinal Cord of the Mouse

By

Nikita Patel

Marie-Claude Perreault

Adviser

An abstract of
a thesis submitted to the Faculty of Emory College of Arts and Sciences
of Emory University in partial fulfillment
of the requirements of the degree of
Bachelor of Science with Honors

Neuroscience & Behavioral Biology

2023

Abstract

Distribution & Density of 5-HT Fibers in the Lumbar Spinal Cord of the Mouse

By Nikita Patel

Serotonergic (5-HT) neurons in the raphe nuclei of the brainstem profusely innervate every part of the central nervous system (CNS) to exert a breadth of modulatory functions, including regulating spinal motor circuits. The existing literature has reported complex and sometimes conflicting actions of 5-HT on spinal motor circuits. This has been attributed to methodological differences (species, age, etc.) and a lack of approaches that would enable the specific activation of the 5-HT raphe neurons projecting to the spinal cord (5-HT raphe-spinal neurons) without activation of the non-5-HT raphe-spinal neurons. Now that such a specific approach is possible in the mouse (Giorgi & Perreault, 2021), it is critical that we gather information about the anatomy of the 5-HT raphe-spinal system in this species. Therefore, this study aims to assess the laminar and funicular distribution and density of 5-HT raphe-spinal fibers projecting to the upper lumbar segments of the spinal cord, where core circuits of hindlimb movements are found, both in newborn mice and in young adult mice. We find approximately 53% more 5-HT axon segments in the ventral horn of the neonate compared to the adult mouse. In addition, we report the ventral and lateral funiculi of the neonate mouse having over three times the number of 5-HT axon segments than the adult mouse. One hypothesis for this large drop in fibers with age is proposed by ten Donkelaar, who suggests redundant axons are selectively reduced following collateralization in the spinal cord.

Distribution & Density of 5-HT Fibers in the Lumbar Spinal Cord of the Mouse

By

Nikita Patel

Marie-Claude Perreault

Adviser

A thesis submitted to the Faculty of Emory College of Arts and Sciences
of Emory University in partial fulfillment
of the requirements of the degree of
Bachelor of Science with Honors

Neuroscience & Behavioral Biology

2023

Acknowledgements

My thanks to Dr. Marie-Claude Perreault for her support and mentorship throughout this project and my time in her laboratory. In addition, thank you to Dr. Astrid Prinz and Dr. Francisco Alvarez for their input on my committee. I would also like to thank Dr. Andrea Giorgi for his assistance in developing this project and Jais Matta for her help in completing my thesis. Lastly, thank you to my mother, Daxa Patel, and close friends for their support as I wrote this thesis.

Table of Contents

Tables and Figures

List of Abbreviations

Abbreviation	Definition
5-HT	Serotonin, 5-hydroxytryptamine
5-HTP	5-hydroxytroptophan
CC	Central canal
ChAT	Choline acetyltransferase
CNS	Central nervous system
DF	Dorsal funiculus
DH	Dorsal horn
DLF	Dorsolateral funiculus
E	Embryonic day
IHC	Immunohistochemistry
INT	Intermediate area
L1	Lumbar cord, segment 1
L2	Lumbar cord, segment 2
L3	Lumbar cord, segment 3
L4	Lumbar cord, segment 4
NeuN	Neuronal nuclei
o/n	Overnight
P	Postnatal day
PBS	Phosphate-buffered saline
PFA	Paraformaldehyde
PPY	Parapyramidal nuclei
SEM	Standard error
RM	Raphe magnus
RO	Raphe obscurus
ROI	Region of interest
RPa	Raphe pallidus
TPH	Tryptophan hydroxylase
TPH2	Tryptophan hydroxylase 2
V4	4^{th} Ventricle
VAChT	Vesicular acetylcholine transferase
VF	Ventral funiculus
VH	Ventral horn
VLF	Ventrolateral funiculus
w/v	Weight by volume

Purpose

In the present study, we examined the distribution and density of 5-HT fibers projecting to the upper lumbar spinal cord at two postnatal ages (P5, P150). We stained against immunoreactive 5-HT fibers and provided a quantitative analysis of their (1) spatial distribution and (2) density in our identified regions of interest: the funiculi and laminae of the L2 spinal segment. We intend to provide a baseline understanding of the maturation of the raphe-spinal 5-HT projections in the mouse by targeting the upper lumbar cord, an area known to be highly innervated by 5-HT fibers in other species. We expect the results to be directly relevant to a pilot study showing that selective optogenetic activation of raphe-spinal projections decreases the firing of lumbar motoneurons induced by the activation of sensory inputs (Giorgi & Perreault, 2021).

Background

Serotonergic (5-HT) Neurons

By profusely innervating every part of the central nervous system (CNS), 5-HT neurons have a breadth of modulatory functions (Hornung, 2003). The 5-HT system has both ascending and descending components, the former targeting the forebrain and the latter innervating every level of the spinal cord. This study will focus on the development of axons, or fibers, arising from the descending system, of which 5-HT has a key role in regulating a range of essential physiological functions such as reflex behaviors, locomotion, and pain modulation (Schmidt & Jordan, 2000; Gackière & Vinay, 2014; Ganley et al., 2022).

Most 5-HT is synthesized in the cell bodies of the raphe nuclei, nine well-circumscribed clusters of neurons distributed rostro-caudally along the brainstem (Dahlström & Fuxe, 1965). 5-HT is generated by modifying the amino acid L-Tryptophan through a two-step reaction mediated by tryptophan hydroxylase (TPH) and 5-hydroxytryptophan (5-HTP) decarboxylase (see **Figure 1**). 5-HT is packaged into synaptic vesicles before it is transported along descending fibers to the spinal cord. 5-HT-producing cells, such as the raphe nuclei, are one of the earliest neuronal types to form in the CNS (ten Donkelaar, 2000). Raphe development occurs during gestation, and by embryonic (E) day 12.5 in the mouse, cells of the caudal raphe nuclei are already identified, with little to no changes in their development by E18.5 (Alonso et al., 2012). Descending 5-HT axons from the raphe originate in the caudal nuclei: the raphe magnus (RM), raphe obscurus (RO), raphe pallidus (RPa), and parapyramidal raphe (PPY) (see **Figure 2**) (Dahlström & Fuxe, 1965).

Figure 1. The biosynthesis of 5-HT consists of two steps: (1) TPH adding a hydroxyl group to L-Tryptophan and (2) 5-HTP decarboxylase removing the carboxyl side chain from 5-HTP.

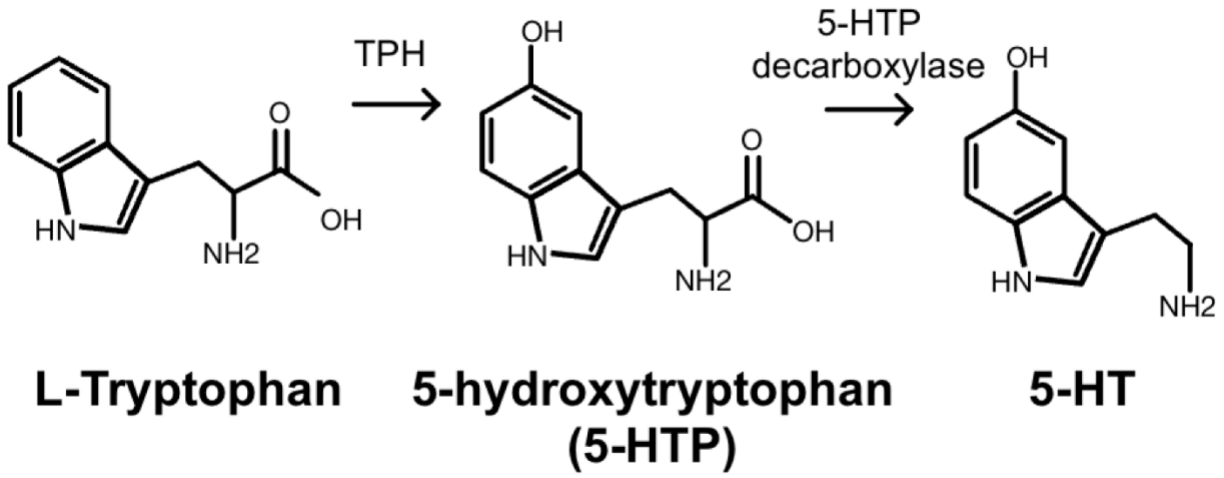

Figure 2. The caudal raphe nuclei in the mouse brainstem. (2A) sagittal view showing RM, RPa, and RO. (2B) transverse view of the RM, RPA, and PPY. The 4th ventricle (V4) is shown for rostrocaudal orientation.

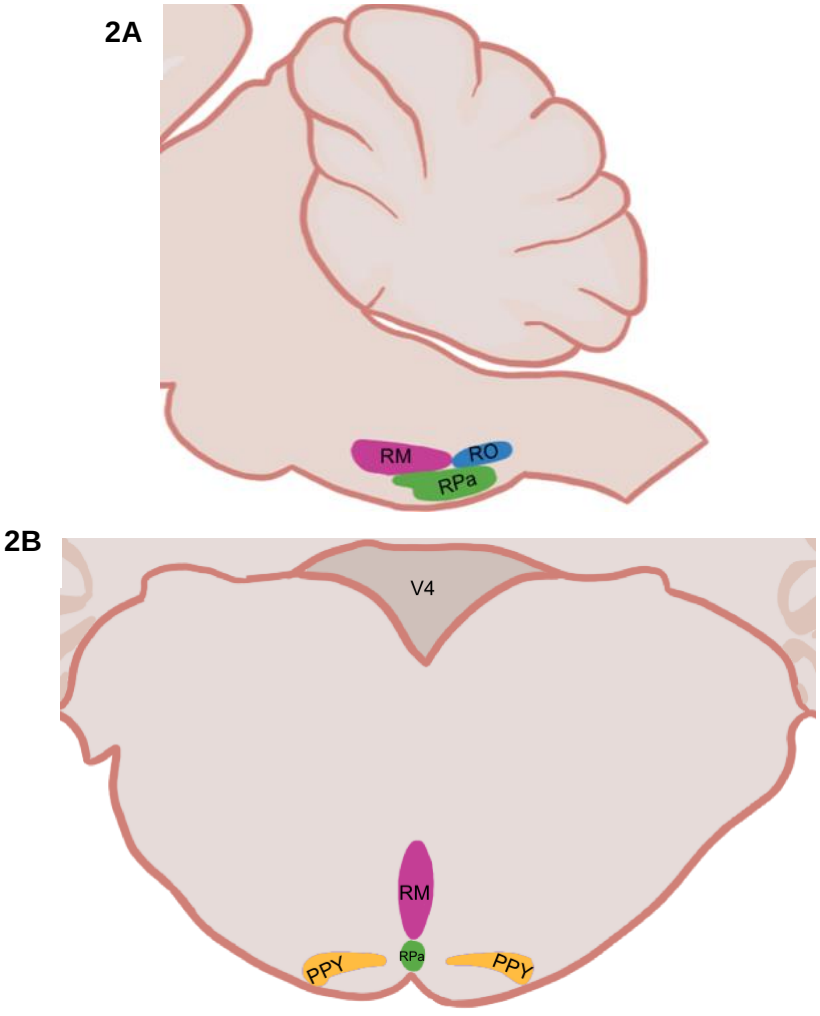

5-HT Fiber Development in the Mouse

5-HT fibers descend to the different levels of the spinal cord in a time-dependent manner. 5-HT fibers reach the cervical cord by E12.5, the thoracic level by E14.5, and the lumbar cord by E16.5 (see **Table 1**) (Ballion et al., 2002). 5-HT fibers first invade the lateral and ventral funiculi of the spinal white matter; this occurs in each level of the spinal cord (Ballion et al., 2002). 5-HT fibers then appear in the ventral and intermediate gray matter of the lumbar cord by postnatal (P) day 0 (Ballion et al., 2002). By P10, 5-HT axons densely invade the entire gray matter of the lumbar cord, and full adult 5-HT maturation is seen (Ballion et al., 2002).

Table 1. Gestational development of the raphe nuclei and its projections in the mouse (Ballion et al., 2002; ten Donkelaar, 2000).

5-HT Fiber Development in the Mouse Spinal Cord				
	Birth of neurons	Descent of 5-HT axons from the raphe		
		Innervation of the cervical cord	Innervation of the thoracic cord	Innervation of the lumbar cord
Raphe Nuclei	E9-E13	E12.5	E14.5	E16.5

5-HT Fiber Morphology

5-HT fibers in the spinal cord have unique morphologies. In both the dorsal and ventral horns, most 5-HT fibers participate in volume transmission; this process involves the release of 5-HT into the extracellular space from varicosities that are not traditional synaptic sites (Hentall et al., 2006; Alvarez et al., 1998). In the intermediate gray matter and ventral horn, 5-HT is also released at traditional axo-dendritic, axo-axonic, and axo-somatic synapses (Privat et al., 1988).

Methods

Perfusion & Tissue Preparation

Mice (n=3 in each group) were anesthetized with Euthasol (Med Vet International; i.p. >100mg/kg) and transcardially perfused. Using a peristaltic pump, we perfused the animals with phosphate-buffered saline (Sigma Aldrich; PBS) and heparin (Med Vet International; 1 unit/mL) followed by 4% paraformaldehyde (Sigma Aldrich; PFA) in accordance with Dr. Perreault's IACUC protocol. After perfusion, the lumbar spinal cord segments were harvested, post-fixed in 4% PFA overnight (o/n), and cryoprotected for at least 24 hours in 30% w/v of sucrose (Sigma Aldrich).

Sectioning

Lumbar (L1-L3) spinal cord segments were embedded in Tissue Tek gel (Electron Microscopy Services) and snap-frozen in liquid nitrogen. The frozen tissue samples were sectioned using a Leica CM1950 Cryostat and collected on charged (+) Superfrost slides. Each L1-L3 sample was cut in the transverse plane with a thickness of 30µm (see **Figure 3**). The sectioned samples were stored at -20℃ until immunohistochemistry procedures were completed.

Figure 3. Segments isolation.

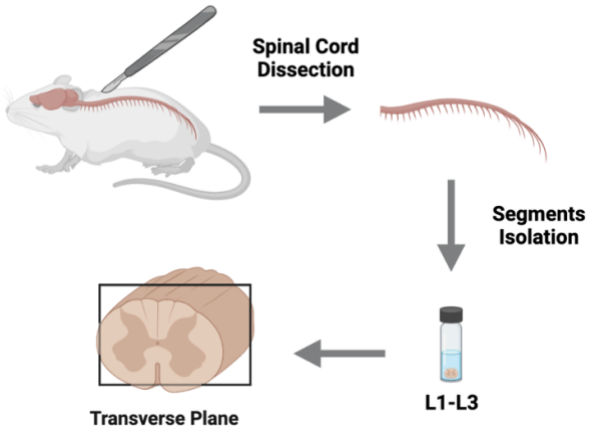

Immunohistochemistry (IHC)

Three IHCs consisting of L2 tissue samples from three adult and three neonate mice in a pairwise fashion were conducted (see **Table 2** for all antibody dilutions and targets). Thus, each IHC pair consisted of sections from one adult and one neonate. All antibodies were diluted in blocking solution consisting of 0.1M PBS 1x (Sigma Aldrich), 0.3% TritonX-100 (Sigma Aldrich), and 5% donkey serum (Jackson Immunoresearch); all washes were done using 0.1M PBS 1X six times, for ten minutes each.

On day one, sections were rinsed with 0.1M PBS 1X before permeabilization and blocking using blocking solution for one hour at room temperature. They were then incubated with rabbit anti-5-HT for 24 hours at 4℃.

On day two, the rabbit anti-5-HT primary antibody solution was carefully decanted from the slides prior to washing. After the washing, the sections were incubated with Cy3 donkey anti-rabbit for two hours in the dark at room temperature. The sections were then washed. After the last wash, the slides were permeabilized and blocked again for one hour at room temperature. The sections were incubated with mouse anti-neuronal nuclei (NeuN) o/n at 4℃.

On day three, the mouse anti-NeuN primary antibody solution was decanted from the slides, and the sections were washed. Sections were then incubated with Cy5 donkey anti-mouse for two hours in the dark at room temperature. After this, the sections were washed, rinsed in distilled H_2O, dried at 37℃ in the dark, and carefully mounted with coverslips using Prolong Antifade Diamond mounting media (Fisher Scientific). All slides were stored at -20℃ until imaging.

Table 2. Antibodies used in final immunohistological procedures.

Antibodies	**Dilution**	**Source**
Rabbit anti-5-HT	1:2,000	Immunostar (20080, lot 1908002)
Mouse anti-NeuN (Biotin Conjugated)	1:250	Millipore (MAB377B, lot NG1899937)
Cy3 donkey anti-rabbit	1:200	Jackson Immuno (7110165-152, lot 138876)
Cy5 donkey anti-mouse	1:200	Invitrogen A10525, lot 1110265)

Imaging & Analysis

Confocal imaging (Olympus FV1000 inverted confocal) was used to visualize hemicords from three sections of each sample. 20X (NA = 0.75) z-stack (z =1.22µm) tiled images were taken of each hemicord using 543nm and 635nm laser lines. Sections from each IHC pair were taken at the same acquisition parameters. Images were later stitched together using ImageJ.

To make axon counts, the white and gray matter of each hemicord were divided into regions of interest. The white matter was sectioned into ventral (VF), ventrolateral (VLF), and dorsolateral (DLF) funicular regions; axon counts covered the entirety of each region. One 100µm x 100µm region of interest (ROI) was selected from the dorsal horn (DH), intermediate area (INT), ventral horn (VH), and central canal (CC) (see **Figure 4** for ROI placement). Axons were manually counted in each ROI per IHC pair.

Figure 4. Reference image displaying ROIs in the gray matter (4A) and the division of the white matter (4B). The DH ROI was taken by drawing a line 50° above the horizontal line which bisected the CC and placing the top right corner at 95% of the length of the line. The CC ROI was centered around the CC. The INT ROI was placed along the horizontal in lamina VII, with the center 30% of the length of the line. The VH ROI was placed along a line 40° below the horizontal, with the center 60% of the length of the line. The division between the VF and VLF was at 30° below the horizontal.

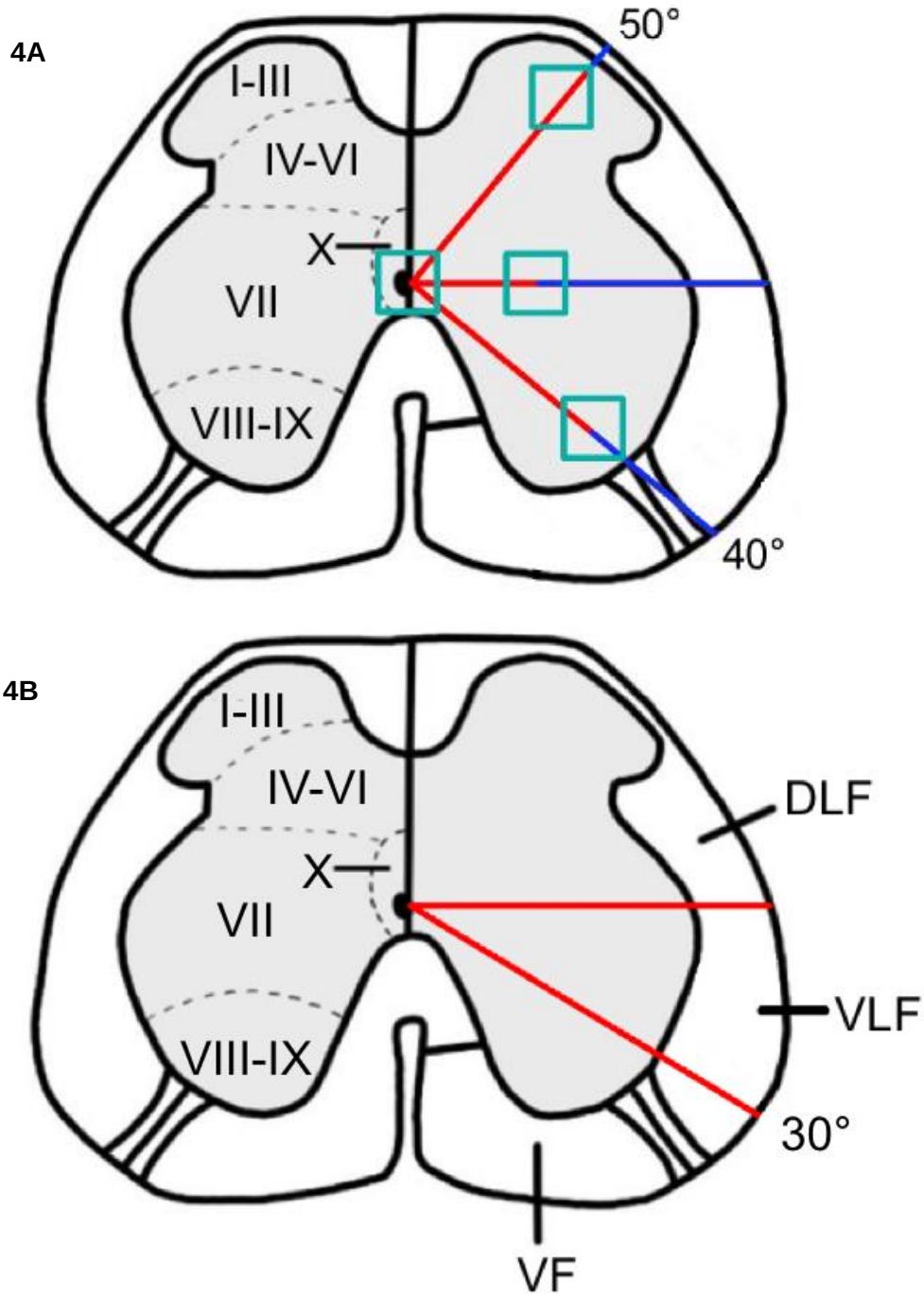

Troubleshooting

Due to high background noise and nonspecific binding, several attempts were made to improve the IHC stain before it was uncovered that some of the secondary antibodies used had been incorrectly stored.

1. Different combinations of primary & secondary antibodies as well as testing multiple dilutions (see **Table 3**).

   We made several attempts to optimize an IHC using rabbit anti-tryptophan hydroxylase 2 (TPH2) to stain against 5-HT fibers and goat anti-choline acetyltransferase (ChAT) to stain against motoneurons. We selected rabbit anti-TPH2 as TPH2 is the rate-limiting enzyme of 5-HT synthesis in the CNS, and we hypothesized that it would be found within 5-HT raphe-spinal fibers. We also were interested in the proximity of 5-HT axons to motoneurons given the nature of the pilot study in the lab. Thus, we attempted to increase our motoneuron labeling by mixing goat anti-ChAT and goat anti-vesicular acetylcholine transporter (VAChT) (Arvidsson et al., 1997). We ultimately could not produce reliable staining using these primary antibodies, changing their respective dilutions, or using antigen retrieval.

2. Antigen retrieval using citrate buffer and heat.

   When tissue is fixed with PFA, protein cross-links form, masking the epitope binding sites for some primary antibodies (Shi et al., 2011). Antigen retrieval is a technique used to uncover epitopes that are masked during the fixation process. We incubated test slides with a citrate buffer at 60℃ to break apart any protein cross-links that may have formed during the fixation process.

After this step, we began a standard IHC, and we evaluated the effect of the binding of our rabbit anti-TPH2 primary antibody. While we did see positive staining of the raphe nuclei using a brainstem sample, we did not see reliable staining using test tissue from the L4 region of the spinal cord.

3. Antigen retrieval using acetone-extracted spinal cord powder.

We attempted to preincubate our FITC donkey anti-rabbit secondary antibody in an acetone powder of mouse spinal cord to eliminate background binding that arose due to shared epitopes with mouse CNS tissue (Ortez et al., 1980). We did not see an improvement in our staining using test L4 tissue, likely due to the incorrect storage of the FITC donkey anti-rabbit secondary antibody.

Table 3. Additional antibodies tested during troubleshooting phase.

Antibodies	**Dilution**	**Source**
Chicken anti-GFP	1:500	Aves (GFP-1020, lot 0511FP12)
Rabbit anti-TPH2	1:500, 1:1,000	Novus Biologicals (NB100-74555, lot D2)
Rabbit anti-TPH2	1:500, 1:1,000	Life Technologies (PA1-778, lot 30483693)
Goat anti-ChAT	1:100	Millipore (AB144P, lot 2500408)
Goat anti-VAChT	1:1,000	Invitrogen (OSV00003G, lot VA2915482)
FITC donkey anti-chicken	1:200	Jackson (703-095-155, lot 119974)
FITC donkey anti-rabbit	1:200, 1:1000	Abcam (AB6798, lot GR174892-5)
Alexa Fluor 488 goat anti-rabbit	1:200	Invitrogen (A11008, lot 1672238)
Cy3 donkey anti-goat	1:200	Abcam (AB6949, lot GR140405)
Alexa Fluor 555 donkey anti-goat	1:200	Abcam (AB150130, lot GR3424827-1)
Alexa Fluor 546 conjugated streptavidin	1:200	Invitrogen (S11225, lot 1736963)

Results

5-HT Fibers in the Gray Matter

The average number of 5-HT fibers in the selected ROIs in the gray matter appears to vary between neonates and adults; however, there is only a statistically significant difference ($p<0.01$; Welch's t-test) in the average number of fibers in the VH ROI of the neonate and the adult (see **Figure 5**). Upon greater examination, it was observed that there was a high density of 5-HT fibers localized around motoneuron pools in the VH (see **Figures 6 & 7**). While the neonate group generally had a higher 5-HT axon count in DH and INT, these results were not significant ($p>0.05$). The adult group had a slightly higher number of average 5-HT axons in the CC region, but this difference was not significant ($p>0.05$).

Figure 5. The average number of 5-HT axon segments in the DH, CC, INT, and VH in three neonate and three adult mice. $p>0.05$ for the DH, CC, and INT area according to Welch's t-test. $p<0.01$ for VH according to Welch's t-test. Error bars represent the SEM and individual dots represent average counts from the three sections from each animal.

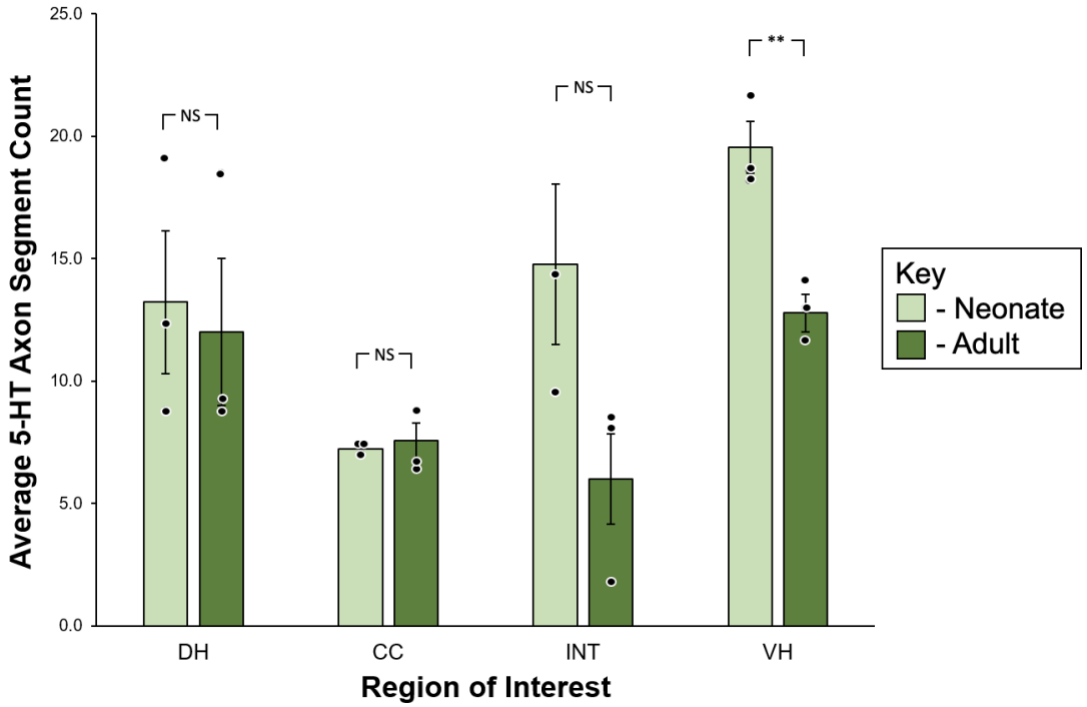

Figure 6. 10X image of full L2 P150 transverse section (6A) with a 40X localized image (6B – 5-HT, 6C – NeuN, 6D – merge) of the ventrolateral horn displaying 5-HT fibers around motoneuron pools.

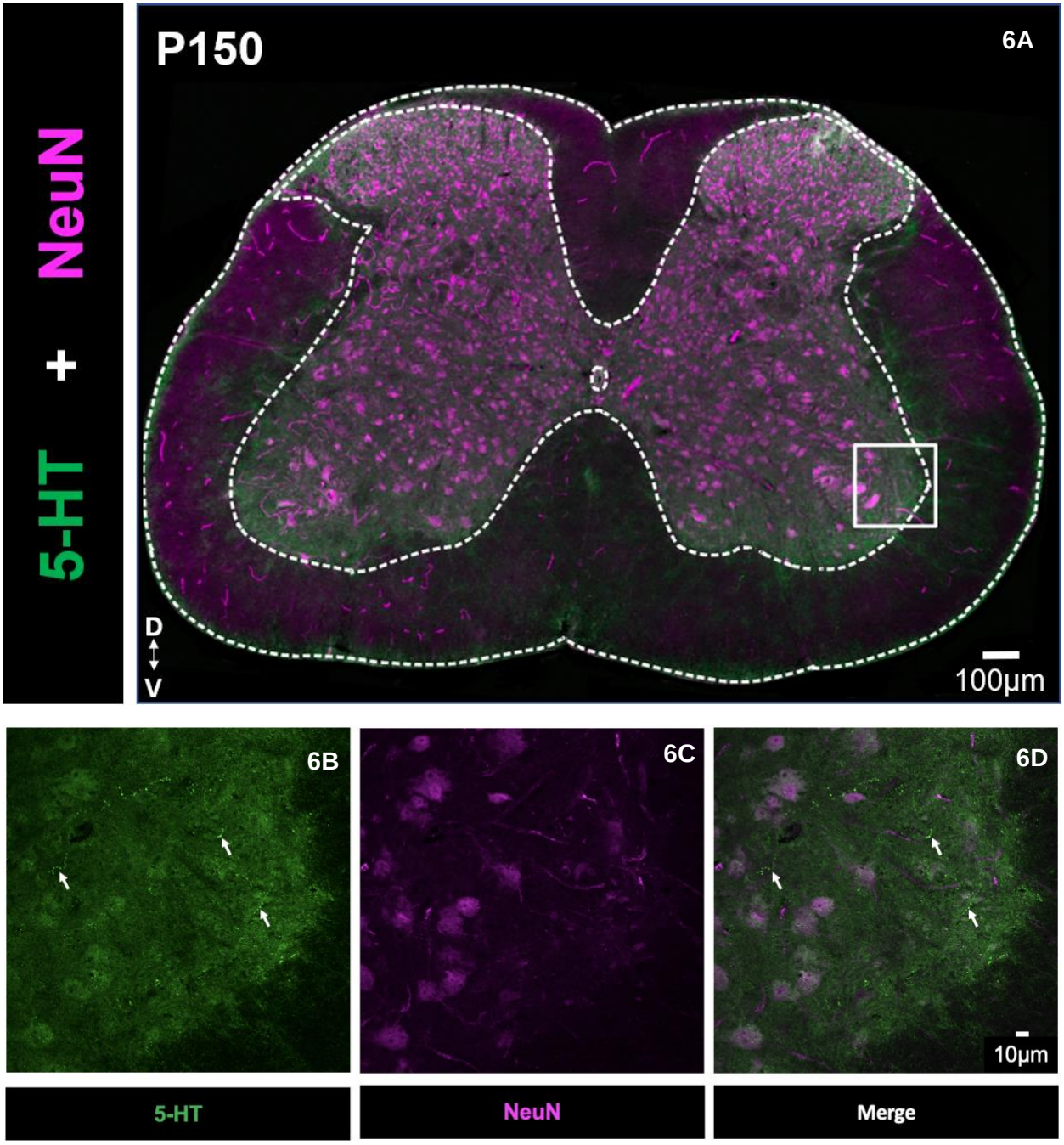

Figure 7. 10X image of full L2 P5 transverse section (7A) with a 40X localized image (7B – 5-HT, 7B – NeuN, 7D – merge) of the ventrolateral horn displaying 5-HT axons around motoneuron pools.

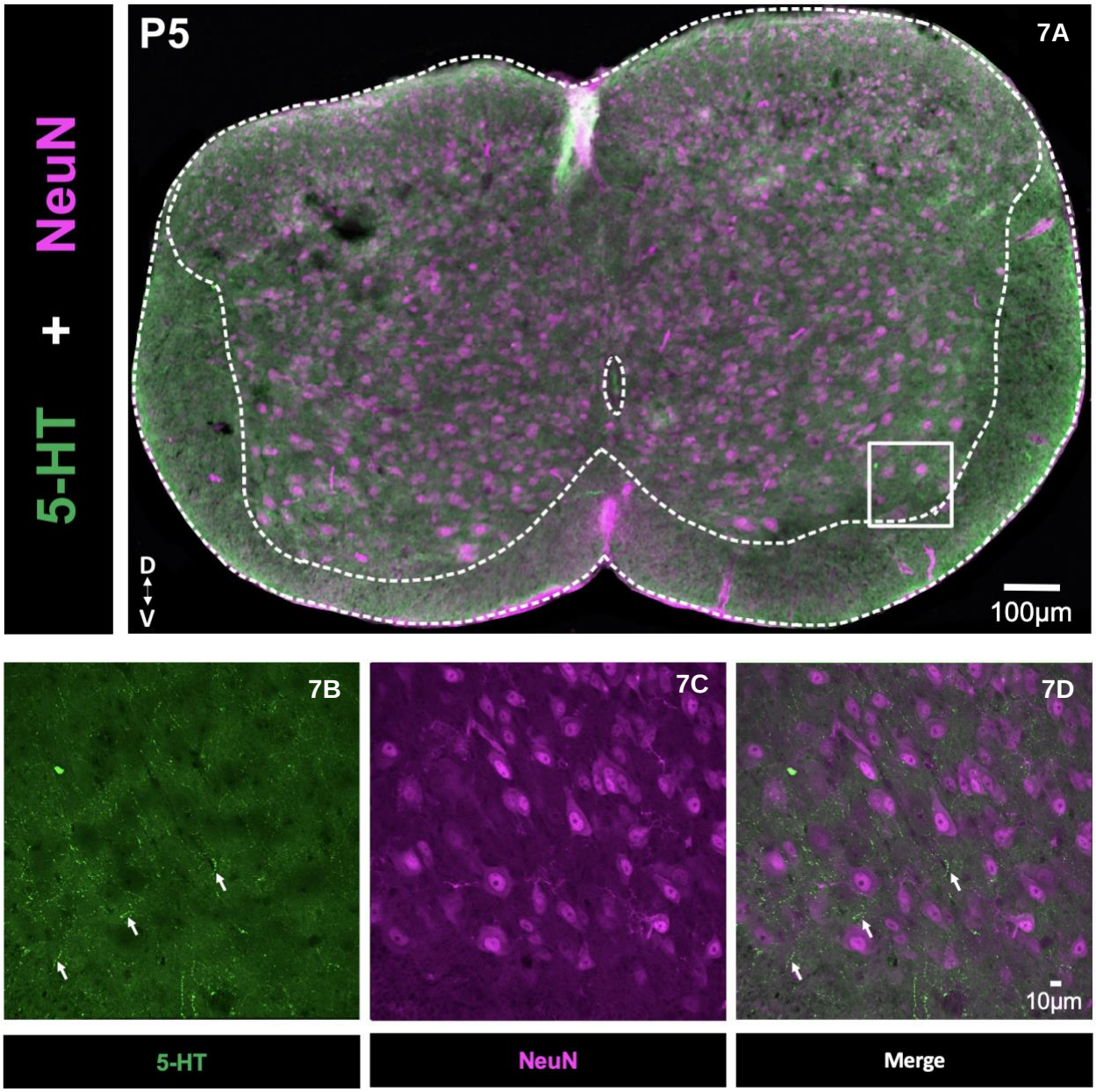

5-HT Fibers in the White Matter

The average number of 5-HT fibers in the white matter is significantly different between neonates and adult mice in all three sections counted ($p<0.05$ for the DLF and $p<0.01$ for the VLF and VF according to Welch's test) (see **Figure 8**). It appears that the neonates had a greater number of 5-HT segments in these regions analyzed. The neonates had an average of 15-20 5-HT axon segments in each section of the funiculi examined, while the adults had an average of 5 5-HT axon segments per ROI.

Figure 8. The average number of 5-HT axon segments in the DLF, VLF, and VF in three neonate and three adult mice. $p<0.05$ for DLF, $p<0.01$ for the VLF, and $p<0.01$ for the VF according to Welch's t-test. Error bars represent the SEM and individual dots represent average counts from three sections from one animal.

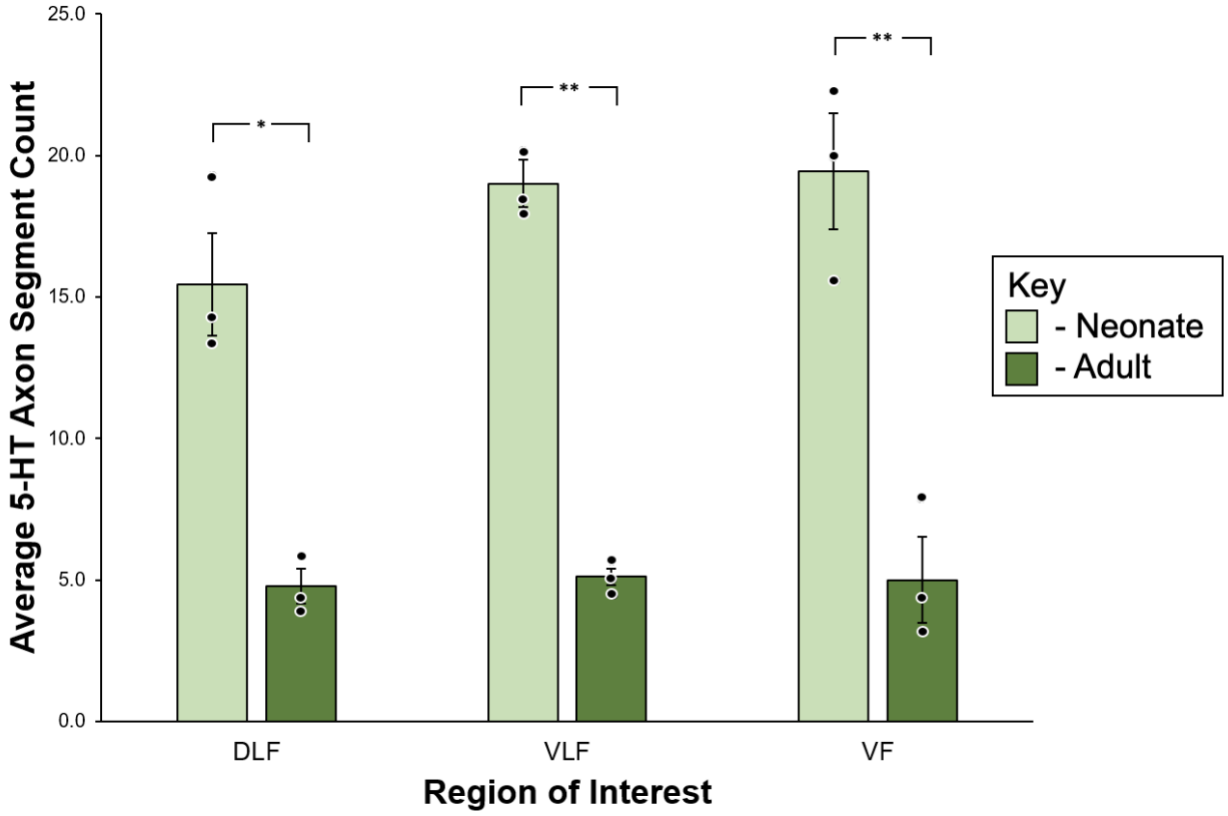

Other Statistical Tests Examined

In addition to the parametric statistics presented earlier, we ran nonparametric statistical tests because it was uncertain if the difference between the two populations followed a normal distribution. We presented the parametric Welch's t-test p-values after evaluating how well distributed the data was around the means and determining the p-values aligned better with the trends seen.

Table 4. Other statistical analyses.

Region	**Wilcoxon Test**	**Wilcoxon-Mann-Whitney Test**	**Welch's T-Test**
DH	p=0.750	p=1.000	p=0.800
CC	p=1.000	p=1.000	p=0.700
INT	p=0.250	p=0.100	p=0.098
VH	p=0.250	p=0.100	**p=0.009**
DLF	p=0.250	p=0.100	**p=0.019**
VLF	p=0.250	p=0.100	**p=0.002**
VF	p=0.250	p=0.100	**p=0.006**

Discussion

Here, we present a novel quantitative analysis of the postnatal distribution and density of 5-HT fibers in the mouse lumbar spinal cord at two distinct ages (P5 and P150). Previous studies documenting the ontogeny and development of 5-HT fibers in the mouse were mainly qualitative in nature, offering observational accounts of the specific time points that the gray and white matter were invaded by descending 5-HT fibers (Ballion et al., 2002).

Decrease in 5-HT Fibers in the Ventral Gray Matter

While we did not note significant differences in the density of 5-HT fibers in the DH, CC, and INT ($p>0.05$) of the gray matter between the two groups, we found a significant difference ($p<0.01$) in the number of 5-HT fibers in the VH, with 53% more axon counts in the neonate compared to the adult group. 5-HT axons are known to proliferate greatly around motoneuron pools in the VH and make direct contact with motoneuron dendrites, which is consistent with 5-HT being a potent neuromodulator of motor control (Alvarez et al., 1998; Cabaj et al., 2016; Madriaga et al., 2004). In the rat, 5-HT fibers are concentrated around motoneuron pools of the ventral horn by P3 (Rajaofetra et al., 1989). The development of the mouse brain, and likewise spinal cord, precedes the rat by 2 days due to differences in gestation time, so it is expected that a high density of 5-HT fibers invades this area early in postnatal development (ten Donkelaar, 2000). This finding is further corroborated by an observation made by Ballion et al. (2002) that 5-HT fibers are found around motoneurons in the ventral horn of the mouse lumbar spinal cord as early as P0.

Decrease in 5-HT Fibers Across the White Matter Funiculi

We report significant differences in the number of 5-HT fibers between the VF ($p<0.01$), VLF ($p<0.01$), and DLF ($p<0.05$) of mice aged P5 and P150 with the neonate group having over three times the number of axon segments in these regions of the white matter than the adult group. The underlying mechanism to explain this phenomenon is unknown and demands further study. We propose a regressive process may underlie this decrease in fibers as mice age. One such mechanism is seen in work done by Chung & Coggeshall (1987) in the dorsal funiculus (DF) of the rat sacral cord, which they define as the region between the two entry points of the dorsal roots. Chung & Coggeshall (1987) report an initial increase in total axon counts in the DF of the rat sacral cord two weeks post-birth (21,000 axons to 26,000 axons), followed by a decrease in the total axon count at full adult maturation (15,000 axons). They further theorize that the axon branching that occurs early in development decreases over time as existing connections strengthen. Notably, their findings are in the DF, while our study focuses on the DLF, VLF, and VF; these regions are implicated in different overall descending tracts and types of control.

The observed decrease in axon segments with age supports a hypothesis proposed by ten Donkelaar (2000), who suggested a series of five steps whereby nearly all supraspinal descending axons innervate the spinal cord. First, axons reach their general targets in the spinal cord. Next, dendrites form and generate specific morphologies. Following this, axons collateralize and develop specific targets prior to the selective reduction of inessential synapses and axonal or dendritic branches. The final step is the fine-tuning of the resulting synaptic connections. The exact timeline of

this process for 5-HT raphe-spinal projections is likewise unknown, but perhaps some axonal collaterals or branches formed early in development are eliminated over time as mice age.

Strengths of Study

A significant strength of this study is the development of a relatively robust and clean IHC for use in the mouse. We employed a three-day procedure and increased the number of washings to reduce the background noise seen during the test IHC phase. In addition, all three IHCs were ran in a semi-parallel fashion to ensure consistency in washing and incubation times since there was a high volume of slides to stain. For example, if the first IHC was started on Monday, the second was started on Tuesday (day 2 of the first IHC), and the third was started on Wednesday (day 3 of the first IHC and day 2 of the second IHC). In addition, all axon counts were made in one sitting, by neonate-adult animal pair, to minimize bias.

Limitations of Study

This study is limited by a few factors in its design. First, there was a small sample size (n=3 for both neonates and adults). The lower power of the study decreases the reliability of the results and demands additional testing to solidify the statistical significance of the observed differences in the density of the 5-HT fibers in L2. In addition, the Cy3 donkey anti-mouse secondary antibody also appeared to stain blood vessels in most animals, indicating the animals may not have been as well perfused as originally thought. Furthermore, ROIs in the gray matter were selected using the same criteria across animal samples, but they may not have been consistently representative of the lamina they corresponded to. For example, the ROI in the intermediate area was

consistently placed in lamina 7, yet some ROIs had zero 5-HT fibers while other regions of lamina 7 of the same animal did appear to have fibers. When extending the study, the number of ROIs in each area of interest (DH, CC, INT, and VH) should be increased to have a more robust count. Moreover, the adult spinal cord is larger than the neonate spinal cord, yet the sizes of our ROIs were not scaled to account for this difference. Future analyses should measure the length and width of each spinal cord and scale the ROIs accordingly. Lastly, due to time constraints, the manual axon count was not blind, and it was conducted by only one individual without an additional counter to double-check the accuracy of the count. Future studies should recruit additional "counting" person who is not affiliated with the acquisition of images or staining process to eliminate any potential counting bias.

Future Directions

A high density of 5-HT fibers was noted around motoneuron pools in the VH of the spinal cord in both neonates and adults. 5-HT is implicated as a potent neuromodulator of motoneurons (Madriaga et al., 2004; Cabaj et al., 2016). In addition to the suggestions noted above, a future study may include an anti-synapsin primary antibody to label synapses and determine if there is synaptic contact between the fibers and motoneurons since previous studies indicate there are 5-HT receptors on motoneurons (Loy et al., 2020). Furthermore, it would be interesting to evaluate any differences in morphology between neonate and adult 5-HT fibers in the spinal cord using 3D microscopy in both the longitudinal and transverse planes since only the transverse plane was examined in this present study. One may analyze any differences in axon diameter and the circumference and distribution of the varicosities along the

fibers at the two postnatal ages (P5 & P150). This would help determine if axons with fewer synapses, and perhaps no longer considered essential, undergo elimination during development as proposed by ten Donkelaar.

References

Alonso, A., Merchán, P., Sandoval, J. E., Sánchez-Arrones, L., Garcia-Cazorla, A., Artuch, R., Ferrán, J. L., Martínez-de-la-Torre, M., & Puelles, L. (2012). Development of the serotonergic cells in murine raphe nuclei and their relations with rhombomeric domains. *Brain Structure and Function*, *218*(5), 1229–1277. https://doi.org/10.1007/s00429-012-0456-8

Alvarez, F. J., Pearson, J. C., Harrington, D., Dewey, D., Torbeck, L., & Fyffe, R. E. W. (1998). Distribution of 5-hydroxytryptamine-immunoreactive boutons on α-motoneurons in the lumbar spinal cord of Adult Cats. *The Journal of Comparative Neurology*, *393*(1), 69–83. https://doi.org/10.1002/(sici)1096-9861(19980330)393:1<69::aid-cne7>3.0.co;2-o

Arvidsson, U., Riedl, M., Elde, R., & Meister, B. (1997). Vesicular acetylcholine transporter (VAChT) protein: A novel and unique marker for cholinergic neurons in the central and Peripheral Nervous Systems. *The Journal of Comparative Neurology*, *378*(4), 454–467. https://doi.org/10.1002/(sici)1096-9861(19970224)378:4<454::aid-cne2>3.0.co;2-1

Ballion, B., Branchereau, P., Chapron, J., & Viala, D. (2002). Ontogeny of descending serotonergic innervation and evidence for intraspinal 5-HT neurons in the mouse spinal cord. *Developmental Brain Research*, *137*(1), 81–88. https://doi.org/10.1016/s0165-3806(02)00414-5

Cabaj, A. M., Majczyński, H., Couto, E., Gardiner, P. F., Stecina, K., Sławińska, U., & Jordan, L. M. (2016). Serotonin controls initiation of locomotion and afferent

modulation of coordination via 5-HT7 receptors in adult rats. *The Journal of Physiology*, *595*(1), 301–320. https://doi.org/10.1113/jp272271

Chung, K. S., & Coggeshall, R. E. (1987). Postnatal development of the rat dorsal funiculus. *The Journal of Neuroscience*, *7*(4), 972–977. https://doi.org/10.1523/jneurosci.07-04-00972.1987

Fuxe, K., & Dahlstöm, A. (1965). Evidence for the existence of monoamine neurons in the central nervous system. *Acta Physiologica Scandinavica*, *62*. https://doi.org/10.1007/bf00337069

Gackière, F., & Vinay, L. (2014). Serotonergic modulation of post-synaptic inhibition and locomotor alternating pattern in the spinal cord. *Frontiers in Neural Circuits*, *8*, 1–7. https://doi.org/10.3389/fncir.2014.00102

Ganley, R. P., de Sousa, M. M., Werder, K., Öztürk, T., Mendes, R., Ranucci, M., Wildner, H., & Zeilhofer, H. U. (2023). Targeted anatomical and functional identification of antinociceptive and pronociceptive serotonergic neurons that project to the spinal dorsal horn. *ELife*, *12*. https://doi.org/10.7554/elife.78689

Giorgi A and Perreault M-C (2021) Optogenetic activation of 5-HT neurons in the raphe pallidus: effect on sensory-evoked responses in lumbar motoneurons of the neonatal mouse. Neuroscience Meeting Planner, Society for Neuroscience, Online Program.

Hentall, I. D., Pinzon, A., & Noga, B. R. (2006). Spatial and temporal patterns of serotonin release in the rat's lumbar spinal cord following electrical stimulation of the nucleus Raphe Magnus. *Neuroscience*, *142*(3), 893–903. https://doi.org/10.1016/j.neuroscience.2006.06.038

Hornung, J.-P. (2010). CHAPTER 1.3 - The Neuronatomy of the Serotonergic System. In B. L. Jacobs & Müller Christian P. (Eds.), *Handbook of the behavioral neurobiology of serotonin* (Vol. 21, pp. 51–64). Elsevier.

Loy, K., Fourneau, J., Meng, N., Denecke, C., Locatelli, G., & Bareyre, F. M. (2020). Semaphorin 7a restricts serotonergic innervation and ensures recovery after spinal cord injury. *Cellular and Molecular Life Sciences*, *78*(6), 2911–2927. https://doi.org/10.1007/s00018-020-03682-w

Madriaga, M. A., McPhee, L. C., Chersa, T., Christie, K. J., & Whelan, P. J. (2004). Modulation of locomotor activity by multiple 5-HT and dopaminergic receptor subtypes in the neonatal mouse spinal cord. *Journal of Neurophysiology*, *92*(3), 1566–1576. https://doi.org/10.1152/jn.01181.2003

Ortez, R. A., Sikes, R. W., & Sperling, H. G. (1980). Immunohistochemical localization of cyclic GMP in goldfish retina. *Journal of Histochemistry & Cytochemistry*, *28*(3), 263–270. https://doi.org/10.1177/28.3.6243683

Privat, A., Mansour, H., & Geffard, M. (1988). Transplantation of fetal serotonin neurons into the transected spinal cord of adult rats: Morphological development and functional influence. *Progress in Brain Research*, *78*, 155–166. https://doi.org/10.1016/s0079-6123(08)60278-2

Rajaofetra, N., Sandillon, F., Geffard, M., & Privat, A. (1989). Pre- and post-natal ontogeny of serotonergic projections to the rat spinal cord. *Journal of Neuroscience Research*, *22*(3), 305–321. https://doi.org/10.1002/jnr.490220311

Schmidt, B. J., & Jordan, L. M. (2000). The role of serotonin in reflex modulation and locomotor rhythm production in the mammalian spinal cord. *Brain Research Bulletin*, *53*(5), 689–710. https://doi.org/10.1016/s0361-9230(00)00402-0

Shi, S.R., Shi, Y., & Taylor, C. R. (2011). Antigen retrieval immunohistochemistry. *Journal of Histochemistry & Cytochemistry*, *59*(1), 13–32. https://doi.org/10.1369/jhc.2010.957191

ten Donkelaar, H. J. (2000). *Development and regenerative capacity of descending supraspinal pathways in tetrapods: A comparative approach*. Springer.